MOMENT-RESISTING STEEL SUBASSEMBLAGES UNDER SEISMIC LOADINGS

by

E. P. Popov[I], V. V. Bertero[II], and H. Krawinkler[III]

SYNOPSIS

A typical subassemblage of a moment-resisting building frame may be idealized by a vertical column that extends to its points of inflection above and below the joint at which horizontal beams are attached. A facility for testing half-scale models of such subassemblages has been developed in which a large axial load can be applied to the column simultaneously with additional vertical loads on the beams. A provision is also made for simulating quasi-statically the effect of the horizontal inertia forces induced by an earthquake. This is done by moving the base of the column back and forth as the outer ends of the horizontal beams freely move horizontally on rollers. In this paper the principal results of fourteen experiments with such structural steel subassemblages are summarized. Hysteretic behavior of these structural systems and their components is illustrated. The $P\delta$ effect and the behavior of plastic hinges in columns under cyclic loads are discussed.

INTRODUCTION

A typical moment-resisting structural steel building frame consists of vertical columns and horizontal beams such as shown in Fig. 1(a). During an earthquake such a structure is subjected to rapidly changing ground acceleration. Neither the intensity nor the duration of a seismic distrubance is known a priori. The problem is entirely nondeterministic, and an experimental program can provide only some bounds of the structural behavior under a variety of loading conditions. Fortunately, in contrast to the rapidly changing ground motion, the structural response of a tall building is relatively slow; and meaningful experiments can be carried out under slowly applied quasi-static loads. This has been the approach pursued in this investigation.

Due to the uncertainties of the possible type of ground motion, two basic types of story force-displacement relationships were investigated. In one, the induced cyclic displacements at the column base were symmetrical with respect to the zero load; in the other, the displacements were deliberately selected to be larger in one direction than in the other. In the first case a sufficiently large number of intense load reversals leads to low-cycle fatigue failure. In the second case, the structure experiences a lateral lurch, and an incremental collapse may occur. The corresponding force-displacement relationships are illustrated in Fig. 1(b). In the experiments described here extreme loading conditions causing inelastic behavior in the specimens were emphasized. Such situations may occur during a severe earthquake. In a sense the experiments reported here may be termed "overtesting," but it is believed that it is essential to know the ultimate load and deformational capacities of steel frames under cyclic loading. A subassemblage fully representative of the interior framing is shown in Fig. 1(c). For the experiments it has been somewhat simplified.

I and II Professor of Civil Engineering, Univ. of Calif., Berkeley, Calif.

III Assistant Research Engineer, Univ. of Calif., Berkeley, California.

SELECTION OF SPECIMENS

The idealized model adopted in this investigation for the interior subassemblages is shown in Fig. 2. It does not fully conform to the subassemblage of Fig. 1(c) but was considered satisfactory. For proportioning of the specimens a 20-story, 4-bay office building designed according to the "allowable stress" philosophy following the general requirements of the 1967 Uniform Building Code and the 1969 AISC specifications served as the prototype [1]. For all specimens $L_1 = L_2 = 160$ in., and $h_a = h_b = 40$ in., meaning that the specimens were scaled down from the prototype in a ratio of 1 to 1.75. The gravity loads $G_1/2$ and $G_2/2$ were applied at third points of the span. In such specimens, the bending moment diagrams due to gravity loads alone are symmetrical, Fig. 3. However, applying the horizontal force H at the movable column base and holding the column top fixed in position results in a sequence of the assymmetric moment diagrams shown in the same figure.

The difference in the bending moments on the two sides of the column occurring under the action of the lateral force H, simulating an earthquake force, induces high shear stresses and distorts the panel zone as shown in Fig. 4. This panel zone distortion may contribute significantly to the story drift. In the usual analyses, rotation of the beam ends and deflection of the column are the two factors commonly recognized in determining the story drifts, whereas the effect of panel deformation is usually ignored. This may lead to a severe underestimate of the story drift, especially when the panel zone is designed according to the working stress philosophy and consequently it may behave highly inelastically when the corresponding beam-column subassemblage is stressed beyond the working stress level Fig. 5. It is to be noted that the moment due to $P\delta$ is additive to the moment caused by H acting with a moment arm h. For large axial column loads and/or story drifts this $P\delta$ effect may become very significant.

In this program fourteen specimens of the type shown in Fig. 2 were fabricated and tested. The main characteristics of the specimens are listed in Table 1. All of the specimens were made of A36 grade steel.

In the experiments the columns of specimens in the A, B, and C series were bent around their strong axes and in series D around their weak axes. The panel zones of specimens A-1 and A-2 were rather weak in shear as the column webs were reinforced only with horizontal stiffeners, whereas A-3 and A-4 were reinforced with doubler plates to minimize shear deformation. In series B the panel zones were completely unreinforced. In this series, the beam depths were varied,but their moment capacity was kept constant. Oversized beams were used in series C to force the occurrence of plastic hinges in columns during cyclic loading. In this series the panel zones were strongly reinforced to minimize their deformation. As noted above, the specimens in the D series were designed for bending columns around their weak axes, and the beams were of sufficient strength to force the occurrence of plastic hinges in the columns.

EXPERIMENTAL PROCEDURE

The setup for testing the subassemblages described above was designed and built at the University of California, Berkeley [2,3,4]. The general

features of this apparatus with a specimen installed in it are shown in Fig. 6. A detailed description of this facility may be found elsewhere [1,3]. Essentially, it consists of a testing frame, loading devices, and instrumentation for measuring loads, displacements, and deformations.

After the specimen is placed in the test frame by means of hydraulic jacks, an axial load up to 600 kips (2,700 kN) can be applied to the column, and simultaneously the beams can be loaded vertically up to 40 kips (178 kN) each. The actual loads are applied by means of hydraulic jacks that pull on distributing beams and, in this manner, deliver concentrated forces at third-points of the beams. This simulates gravity loading. The simulation of the earthquake force is achieved by using a double-acting horizontal jack which can apply cyclic load reversals to the lower column end. The column jack is mounted on a movable cart such that the axial load on the column is always applied vertically. Special gravity load simulators maintain vertical forces on the beams while moving horizontally. In this manner, the specimen can be subjected both to the vertical gravity loads and a selected sequence of horizontally applied cyclic forces.

The complex problem of determining the magnitudes and the load-reversal sequence was resolved by employing two types of cycling programs shown in Fig. 7. In the one type a subassemblage was subjected to a stepladder sequence of column displacements; in the other, large column displacements were made deliberately unsymmetrical with respect to the initial position. It is believed that with these two types of loading histories, bounds on the inelastic behavior of subassemblages indicated in Fig. 1(b) can be established.

Four spool-type aluminum transducers with electrical wire resistance gages were used to measure the loads applied by hydraulic jacks, Fig. 6. Two of these transducers were mounted at gravity load simulators, one on top of the column jack and one for measuring the horizontal force at the bottom of the column. Shear transducers were used to measure the reactions at the outer ends of the beams.

Throughout each experiment the equivalent of gravity loads was maintained; however, the horizontal force applied at the bottom of the column was varied. Continuous automatic records from electric gages were obtained for some data; the remainder was read using a low-speed scanner. As an independent control on the deformations, optical procedures were also employed. Three Wild T2 theodolites were used to measure the movement of column ends and panel zone as well as deflections along the beams. A Wild P30 phototheodolite was used for sequential photographs of a grid system marked on the specimen in and around the panel zone. This dual control system on displacements provided valuable verification of the data. For more details, the reader is referred to Refs. 1 and 3.

EXPERIMENTAL RESULTS

The most important information obtained from these experiments is reflected in the relationship between the lateral force H and the displacement δ of the bottom column hinge. This is best shown on the hysteresis loop diagrams for the entire assemblage. The behavior of the panel zone can be studied from photogrammetric records and from measurements of the average

angle of distortion γ_p^{av} caused by shear deformation. If plastic hinges occur in the columns, their behavior above and below the joint must be differentiated.

Specimens A. In each of these experiments the column's force P was 86 kips (382 kN), and the third-point forces applied through a distributing beam were 6 kips (26.7 kN) each. The magnitude and direction of the horizontal force H was varied as indicated in Fig. 7.

The H-δ diagrams for three of the four specimens are shown in Fig. 8. As specimens A-1 and A-2 were identical, the comparison of these diagrams shows the effect of a different cyclic history. In spite of the extremely severe testing conditions, this effect is seen to be rather mild. The strength of specimens A-1 and A-2 was low because the weak panel did not permit the development of the full strength of the beams. The behavior of A-3 with the panel zone reinforced by a doubler plate is dramatically better. Initially the system is a little stiffer, and later it exhibits substantially higher strength and generates larger hysteresis loops. The specimen A-4 which had two vertical plate stiffeners also performed better than either A-1 or A-2. In the first monotonic cycle this specimen attained strength that was as good as A-3, but at the later stages of cyclic loading its capacity was between that of A-2 and A-4. The reason for the better behavior of A-3 and A-4 is that in both cases the panel zones remained nearly elastic throughout the experiments, and the main inelastic deformations occurred in the beams. The apparent work-softening of the hysteresis loops is due to the Pδ effect.

The deformation pattern at the joint of an A-specimen obtained by photogrammetric technique [1,3] is shown in Fig. 9. This is to be compared with the schematic diagram of Fig. 4. A tendency for initiating cracks in the beam flanges at local kinks was observed in cases where the inelastic shear distortions in the panel were large. Besides the detailed study of shear deformation of the panel zone, the main features of this behavior were obtained by measuring the relative displacements of diagonally opposite corner points of the panel, Fig. 10. This permitted the plotting of the angular panel distortion vs. the difference in bending moments on the two sides of a column resulting in the loops shown in Fig. 11.

In an unreinforced panel of an A-specimen the observed angular distortions of the panel are large, Fig. 11. Doubler plates greatly inhibit this deformation. However, their own deformation lags behind that of the column web, Fig. 12. When the panel zone is reinforced, clearly discernible plastic hinges form in the beams with little inelastic action in the panel zone, Fig. 13.

Specimens B. In the B-specimens the columns were considerably heavier than in the A-specimens, as these subassemblages corresponded to the lower story of the prototype. For these specimens the axial force P was maintained at 339 kips (1,507 kN), and the load on each gravity load transducer was kept at 11.8 kips (52.6 kN). The horizontal force H was varied as in the previous experiments. The H-δ diagrams for three B-specimens are shown in Fig. 14. Since the column webs were heavy, the panel zone deformations were small; and the weak parts of these specimens were the beams in which plastic hinges occurred. This required high rotation capacities of the

beams. In the more compact beams of specimen B-4 the hysteresis loops appear to be stable, as may be judged by their repetitive character even at large displacements. This is not evident for B-1 and B-2 where the lateral instabilities of the beams prevented complete stabilization of the hysteresis loops at large displacements.

The results of photogrammetric analysis for B-2 are presented in Fig. 15 and show a substantially different deformation pattern of the panel zone compared to that of A-2 (see Fig. 10). The difference between these two cases may also be noted from Fig. 16 where the respective shear stress distributions are shown.

Specimens C. The commonly accepted approach for the aseismic design of moment-resisting frames tries to avoid significant inelastic action in the columns; however, this can occur during a severe earthquake. Therefore, it is essential to determine the behavior of the columns under cyclic loading when plastic hinges occur in them. This was the purpose of the C and D series of experiments. In both series of experiments the beams were sufficiently large to force the occurrence of plastic hinges in the columns.

The behavior of columns bent around their strong axes when plastic hinges occur in them was explored in the C series of experiments. Panel zones were heavily reinforced with doubler plates in addition to the horizontal stiffeners, and a wide range of P/P_y ratios was studied. A representative case is that of specimen C-2 for which three sets of H-δ hysteretic loops are shown in Fig. 17. The first H-δ diagram looks ordinary and is of the type encountered in cases with a weak Pδ effect. However, columns in which plastic hinges occur when subjected to severe cyclic loading tend to assume single curvature from top to bottom. The permanent set is such that the columns become and remain C-shaped. As inelastic strains occur on the compression side, the material strain hardens and becomes stronger. Therefore, on a return stroke the column does not fully straighten out, and the single curvature shape becomes progressively more and more pronounced. During cyclic application of the force H the displacement of the panel zone relative to both of the column ends takes place in the same direction but by different amounts. The load-displacement paths between the panel zone and the top as well as the bottom of the column are given in Fig. 17. The relative displacement above the column panel zone is designated by δ_c^a and by δ_c^b for below. The capability of absorbing and dissipating energy by the columns under such severe cycling loadings is encouraging. A photograph of a severely bent column may be seen in Fig. 18.

Specimens D. In some situations the beams may be strong enough to force hinges to occur in the columns when the latter are being bent around their weak axes. This condition under cyclic load was investigated in the D series experiments. Under small lateral force H such columns generated small stable hysteretic loops. However, as the loading progressed, column flanges tended to buckle, Fig. 19; and as with the C specimens, the columns become C-shaped. Here also the column was capable of withstanding significant inelastic deformations before the hysteresis loops become unstable. A photograph of a column at the end of an experiment is shown in Fig. 20.

CONCLUSIONS AND RECOMMENDATIONS

1. Shear distortion of weak panel zones may contribute significantly to the story drift and thereby accentuate the $P\delta$ effect. The importance of this is illustrated in Fig. 21 for specimen A-2. The experimental curve must be modified by $P\delta/h$, as well as by the displacement caused by the shear deformation of the panel zone to obtain agreement with the simple plastic theory. Through proper use of doubler plates, panel zone deformation can be controlled.

2. When panel zones are adequately reinforced, the inelastic deformations are concentrated at critical regions along the beams and/or columns and high rotation capacities may be required in these regions.

3. Steel beams are capable of supplying the required ductility provided that they have compact sections and are adequately braced. In this connection, it must be recognized that the occurrence of local instabilities in the plastic regions is accentuated by cyclic loading. Therefore, the b/t and d/t ratios must be conservatively selected. Since under under the lateral loads the bottom flanges of the beams may be in compression over a considerable length, they must be well braced. For large story drift, the lateral instabilities of the beams may prevent complete stabilization of the hysteresis loops. Hence adequate bracing is essential. The hysteretic behavior of steel beams can be reasonably well predicted on the basis of bi- or tri-linear moment-curvature relationships reported elsewhere [7].

4. Plastic deformation in columns can be tolerated to some extent; however until further research becomes available, the current practice of trying to avoid plastic hinges in columns seems appropriate to preclude abrupt failures.

5. Structural steel as a material behaves very well under reversed loading. Moment-resisting steel frames with strong columns and properly detailed beams and panel zones are capable of dissipating energy in excess of that required even for cases of extreme earthquakes.

ACKNOWLEDGEMENTS AND REFERENCES

The authors are most grateful for the financial support provided over a period of years by the American Iron and Steel Institute which made this work possible. Messrs. L. H. Daniels, A. L. Collin, I. M. Viest, and E. W. Gradt of the above organization, as well as several engineers from the Structural Engineers Association of California deserve special thanks. National Science Foundation support aided in the preparation of this paper and is gratefully acknowledged.

[1] Krawinkler, H., et al., EERC 71-7, UC Berkeley, Oct. 1971.
[2] Popov, E. P., et al., RILEM Symposium, Bucharest, Sept. 1969.
[3] Bertero, V. V. and Popov, E. P., Experimental Mechanics, Aug. 1971.
[4] Bertero, V. V., et al., J. Struct. Div. ASCE, May 1972.
[5] Yamada, M., et al., Der Stahlbau, Vol. 3, March 1971.
[6] Igarashi, S., et al., Trans. A.I.J., Nos. 169 and 170, April 1970.
[7] Popov, E. P., IABSE Symposium, Lisbon, 1973, in press.
[8] ASCE Manual No. 41, 1971.

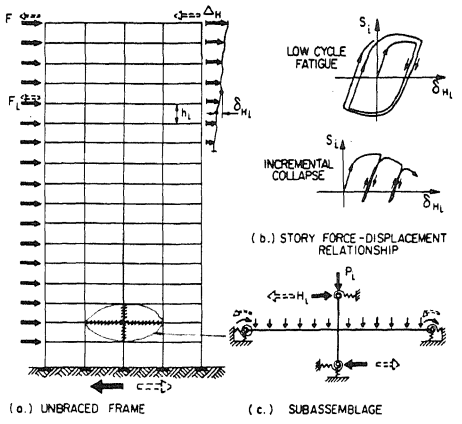

Fig. 1. Moment-Resisting Frame

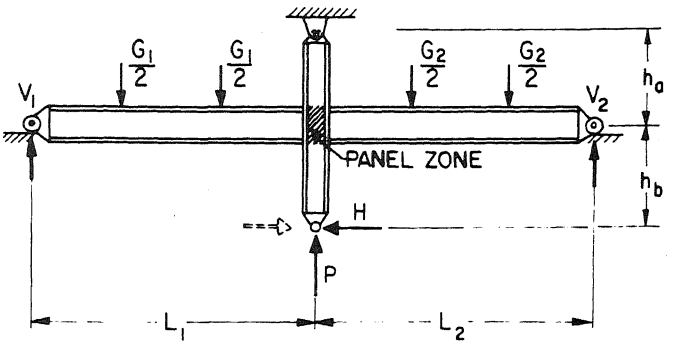

Fig. 2. Idealized Subassemblage

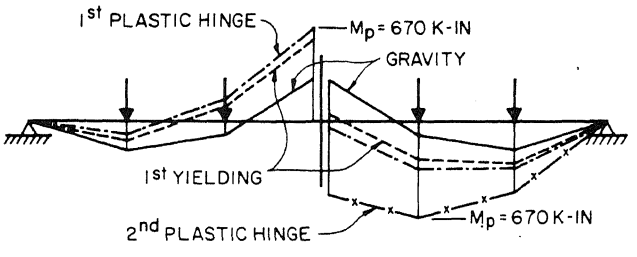

Fig. 3. Bending Moment Diagrams

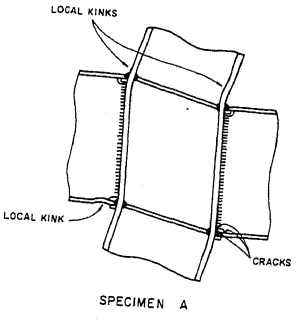

Fig. 4. Panel Zone

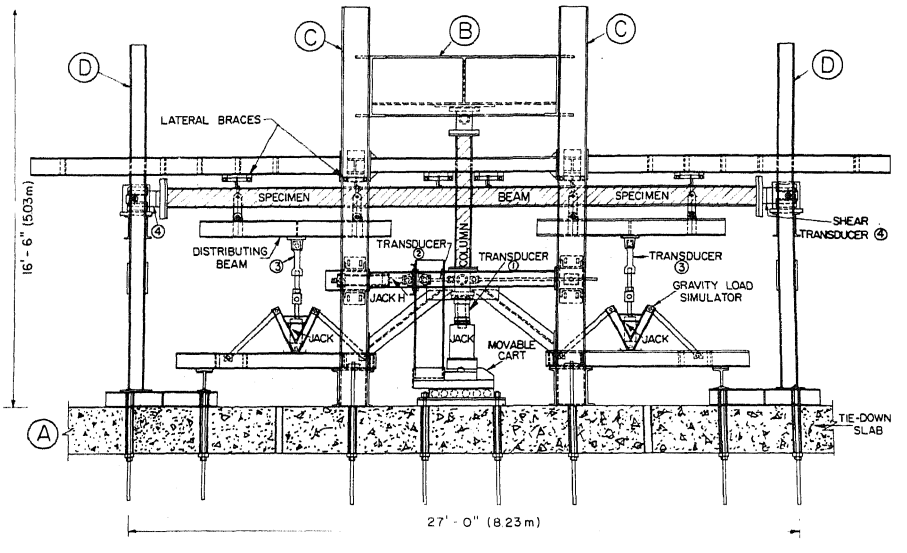

Fig. 6. General Experimental Setup

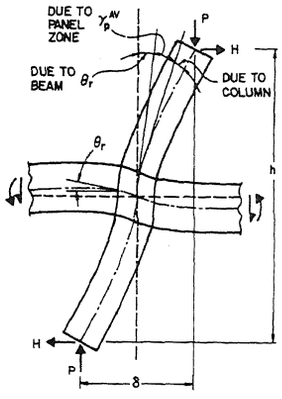

Fig. 5. Components of Story Drift

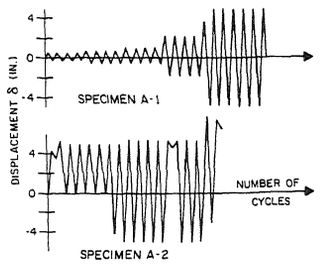

Fig. 7. Cycling Programs

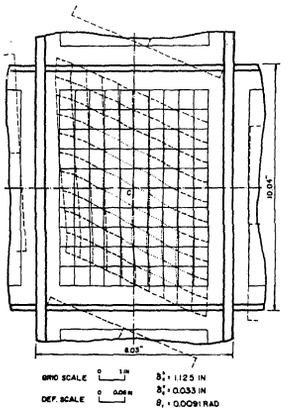

Fig. 9. Panel Zone

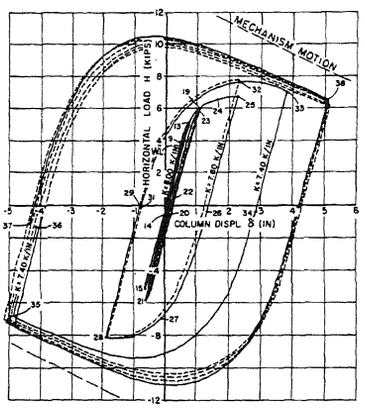

SPECIMEN A-1

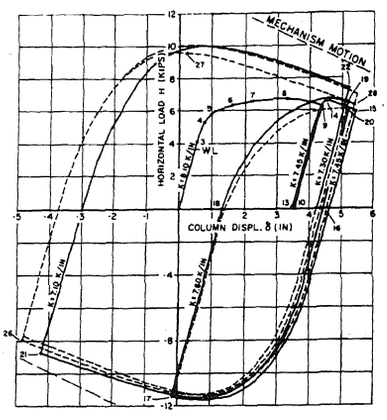

SPECIMEN A-2

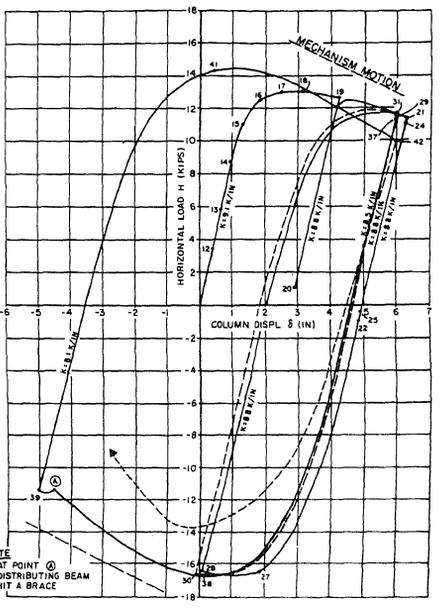

SPECIMEN A-3

Fig. 8. H-δ Hysteresis Diagrams

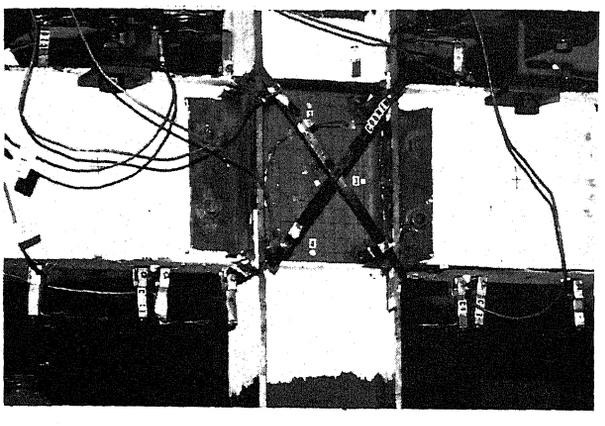

Fig. 10.

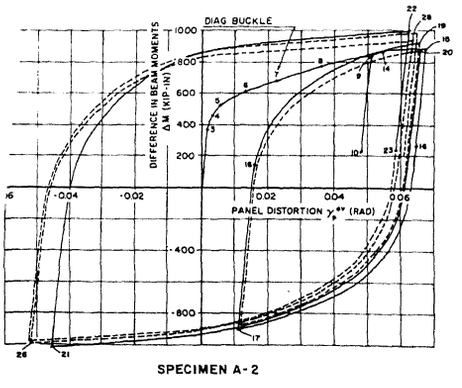

SPECIMEN A-2

Fig. 11. Δ M vs. γ

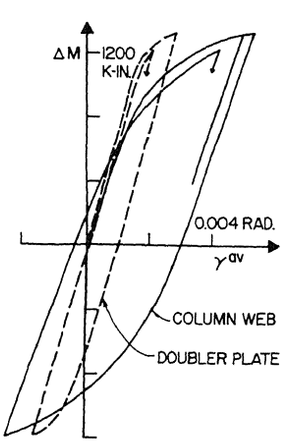

SPECIMEN A-4 Fig. 12.

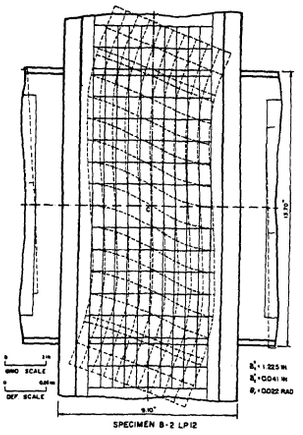

Fig. 15.

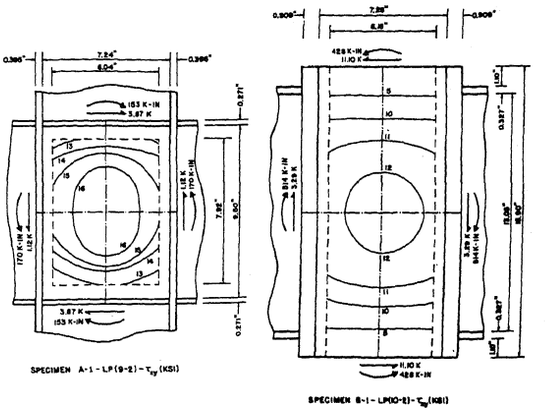

Fig. 16.

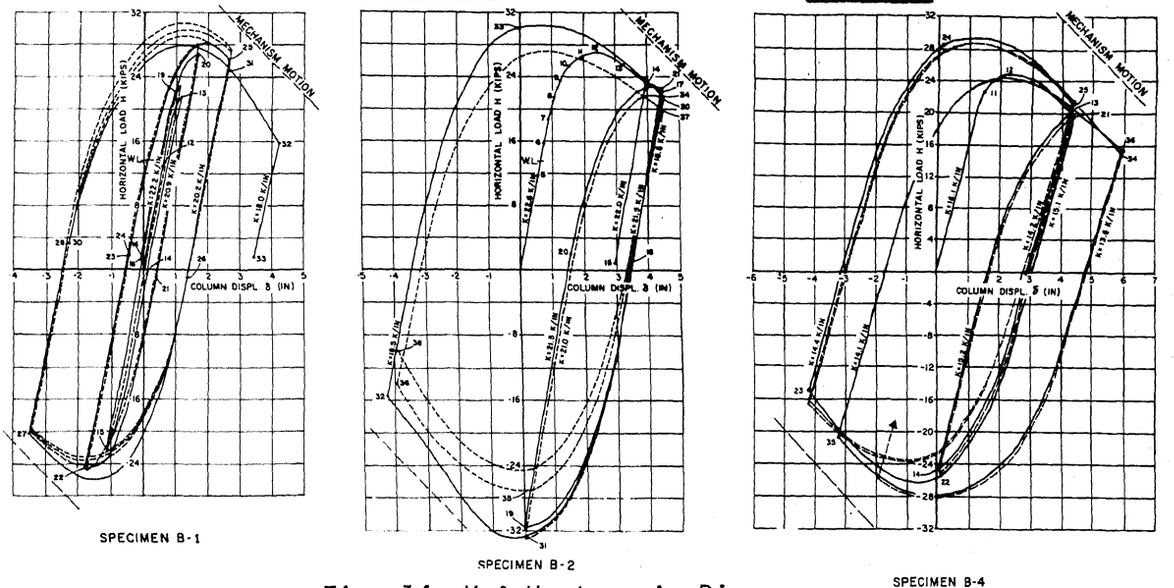

Fig. 14. H-δ Hysteresis Diagrams

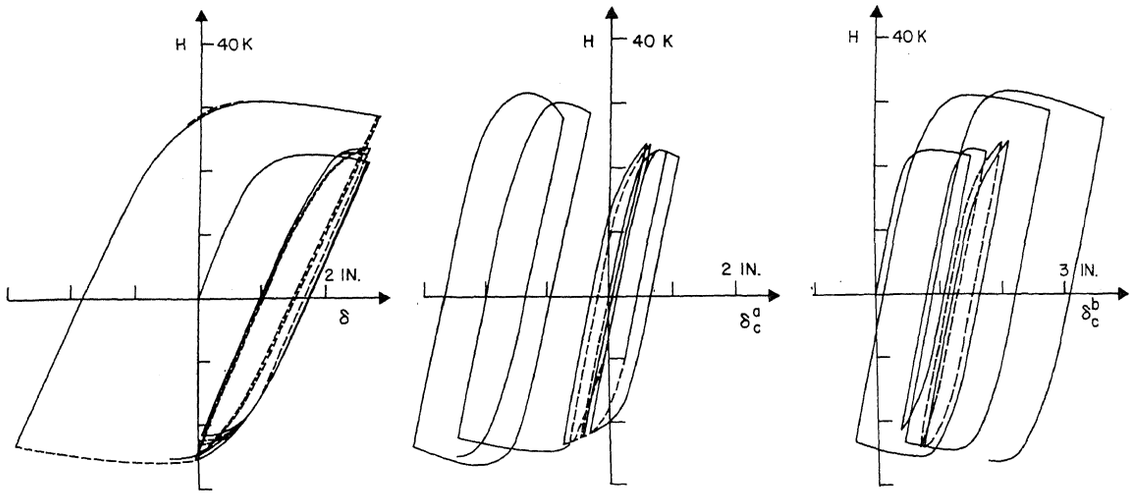

Fig. 17. Specimen C-2; $P/P_y = 0.6$

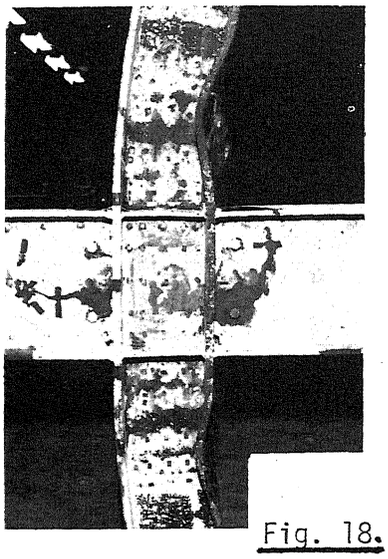

Fig. 18.

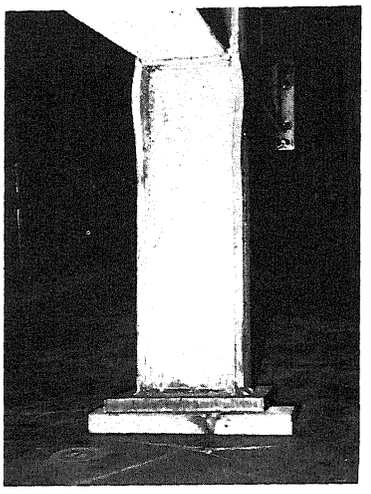

Fig. 19.

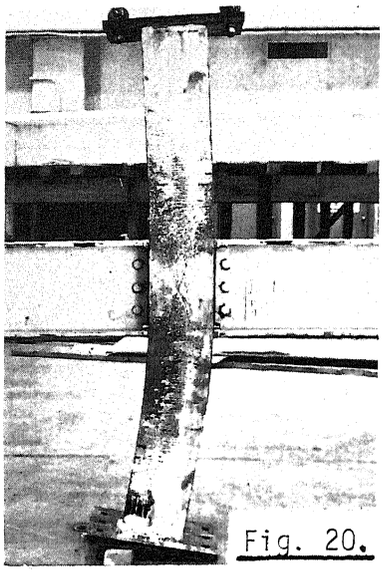

Fig. 20.

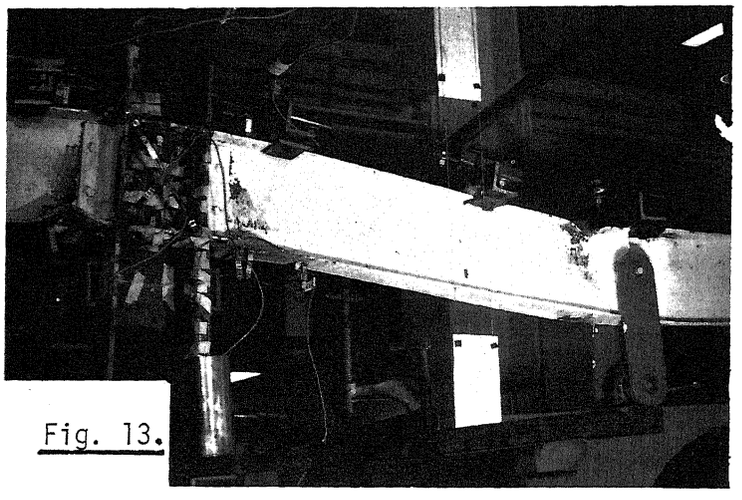

Fig. 13.

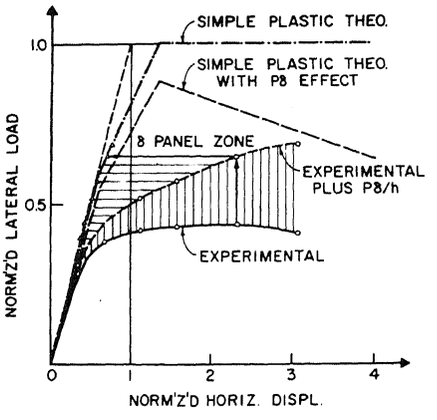

Fig. 21.

Table 1. CHARACTERISTICS OF SPECIMENS

Specimen No.	Beam Size	$\frac{b}{t}$	Column Size	$\frac{P}{P_y}$	Panel Reinforcement (Type)
A-1	B 10 x 15	14.9	W 8 x 24[a]	0.36[b]	Horizontal Stiffeners
A-2	B 10 x 15	14.9	W 8 x 24[a]	0.36[b]	Horizontal Stiffeners
A-3	B 10 x 15	14.9	W 8 x 24[a]	0.36[b]	Horizontal Stiffeners; One 0.25 in. doubler plate
A-4	B 10 x 15	14.9	W 8 x 24[a]	0.36[b]	Two vert. 0.25 in. plates (Box section)
B-1	B 14 x 22	15.3	W 8 x 67	0.48[b]	None
B-2	B 14 x 22	15.5	W 8 x 67	0.48[b]	None
B-3	W 12 x 27	11.7[c]	W 8 x 67	0.48[b]	None
B-4	W 10 x 29	10.25[d]	W 8 x 67	0.48[b]	None
C-1	W 12 x 31	14.0	W 8 x 48	0.80[b]	Horizontal Stiffeners; Two 0.25 in. doubler plates
C-2	W 12 x 31	14.0	W 8 x 48	0.60[b]	Horizontal Stiffeners; Two 0.25 in. doubler plates
C-3	W 12 x 31	14.0	W 8 x 48	0.50[b]	Horizontal Stiffeners; Two 0.375 in. doubler plates
C-4	W 12 x 31	14.0	W 8 x 28	0.30[b]	Horizontal Stiffeners; Two 0.375 in. doubler plates
D-1	W 12 x 31	14.0	W 8 x 48	0.50[b]	(Welded flanges; bolted webs)
D-2	W 12 x 31	14.0	W 8 x 48	0.30[b]	(Welded flanges; bolted webs)

a. Flanges milled to 5.82 in. to simulate section of prototype.

b. P_y is based on 36 ksi yield strength.

c. Flanges milled to 4.71 in.

d. Flanges milled to 4.93 in.